

N6319176



# TECHNICAL NOTE

D-1619

EFFECTS OF DISPLAY NOISE ON PILOT CONTROL OF THE  
TERMINAL PHASE OF SPACE RENDEZVOUS

By Jack E. Pennington

Langley Research Center  
Langley Station, Hampton, Va.

NATIONAL AERONAUTICS AND SPACE ADMINISTRATION  
WASHINGTON

August 1963

NASA TN D-1619

LIBRARY

National Aeronautics and Space Administration

# NATIONAL AERONAUTICS AND SPACE ADMINISTRATION

---

## TECHNICAL NOTE D-1619

---

### EFFECTS OF DISPLAY NOISE ON PILOT CONTROL OF THE TERMINAL PHASE OF SPACE RENDEZVOUS

By Jack E. Pennington

#### SUMMARY

One method proposed for completing the terminal phase of space rendezvous is to place the ferry vehicle on a collision course with the space station and then hold the course while reducing the range and range rate to zero. The course can be achieved by arresting the rotation of the line of sight to the station. This tracking task has been simulated previously, both visually and with perfect radar assumed in the cockpit instrumentation. The series of tests described in the present paper was made to determine the pilot's ability to complete the rendezvous maneuver in the presence of display noise.

The output of a random-noise generator was inserted into the instrument display to introduce an error signal similar to that which could be expected from a radar system. Runs were made first with perfect instruments and then with the noise error introduced into the data displays.

Results show an increase in fuel consumption and time needed to complete the mission, and a decrease in pilot assurance, with the noise error in the instrument. Pilot proficiency increased with an increase in the accuracy of the display instruments and decreased with an increase in the amplitude of the error signal.

#### INTRODUCTION

It has been shown in reference 1 that a pilot can successfully effect rendezvous by using simple optical devices and manual procedures. Previous simulations with the assumption of noise-free instrument displays from "perfect" radar and auxiliary electronic systems have also shown that the pilot can perform satisfactory rendezvous operations (ref. 2). The procedures involved in using such equipment are, in fact, less complicated than the visual-manual procedures. The use of perfect instrumentation would reduce the pilot's workload, but the visual methods would still remain available as backup in case of equipment failure. Available instrumentation is not perfect, however, and it is desirable to know how imperfections such as radar noise affect the pilot's control capability.

Radar ranging systems can be used to obtain range, range rate, the angles between the line of sight and a set of fixed axes in the space station, and the rate of change of the line-of-sight angles. The inherent radar error in any of these measurements could have been investigated, but the error in the line-of-sight angle rates was chosen because (1) the performance of the entire rendezvous maneuver depends upon the use of these data in achieving an early interception course, (2) at the start of the maneuver, when it is necessary to obtain the course as soon as possible, the angular rates are very small, and (3) the small rate signal causes a large noise-to-signal ratio, making the noise particularly apparent on the sensitive cockpit instrument.

The radar noise was simulated by a random noise generator whose output was combined with the line-of-sight angle signal. The combined quantities were then differentiated and fed from the computer to the angular-rate display meter in the cockpit. All other instruments were assumed to be perfect.

This series of tests was designed to be a brief exploratory investigation to determine whether pilot performance was impaired and, if so, to what extent. The noise was placed at a rather severe level to show the effects in an extreme case. Though an effort was made to correlate the noise level and spectrum with available radar data, these data do not represent the current state of the art.

#### SYMBOLS

The English system of units is used in this study. In case conversion to metric units is desired, the following relationships apply: 1 international foot = 0.3048 meter, and 1 international nautical mile = 1,852 meters.

$F_X, F_Y$	force along the X and Y body axes, respectively, g units
R	range, distance along line of sight from space station to ferry, international nautical miles or international feet
s	variable in Laplacian form
t	time, sec
X, Y, Z	principal body axes of ferry vehicle
$X_i, Y_i, Z_i$	inertial axes referred to space station
$x_i, y_i, z_i$	coordinates along $X_i$ -, $Y_i$ -, and $Z_i$ -axis
$\alpha$	angle subtended by line of sight between space station and ferry vehicle and projection of line of sight in $X_i Y_i$ -plane, deg
$\beta$	angle between $X_i$ -axis and projection of line of sight in $X_i Y_i$ -plane, deg

$\lambda$	autocorrelation function, volts <sup>2</sup>
$\sigma$	rms value of noise, volts
$\tau$	time constant obtained in feedback system, sec
$\Phi$	power spectral density, volts <sup>2</sup> -sec
$\phi, \theta, \psi$	roll, pitch, and yaw angles, respectively, deg
$\omega$	frequency, radians/sec

#### Subscripts:

R	radar
G	noise generator

A dot over a quantity denotes the first derivative with respect to time.

### EQUIPMENT

#### Cockpit Display

The same equipment and procedures were used in both the noise and no-noise tests. The simulator consisted of a fixed-base cockpit, instrument panel, rudder treadles, side-arm controller, and on-off thrust buttons. The cockpit and instrument panel are shown in figures 1 and 2.

Line-of-sight angles  $\alpha$  and  $\beta$  were presented on separate meters. Roll and pitch displacements  $\phi$  and  $\theta$  were shown on a two-axis eight-ball, while yaw angle  $\psi$  was on the same type of instrument as  $\alpha$  and  $\beta$ . Line-of-sight angular rates ( $\dot{\alpha}$  and  $\dot{\beta}$ ) were presented on the double-needle meter at the top of the instrument panel. The  $\dot{\alpha}$  needle was hinged at the left and the  $\dot{\beta}$  needle at the top. Initially, full-scale deflection of either needle indicated a rate of 1.5 milliradians/sec; however, the sensitivity was decreased at close ranges to one-tenth its original value. This was necessary because the line-of-sight rate is inversely proportional to range, and at close ranges signals could overdrive the meter if sensitivity were not reduced.

#### Computer Program

A set of inertial axes, with the origin at the center of the earth and with the space station orbiting in the  $X_1Z_1$ -plane, was assumed. The forces assumed to be acting on the ferry were thrust in both directions along the longitudinal (X) and lateral (Y) body axes, and gravity. In order to present the data to the pilot in a usable form, it was necessary to convert from the body-axis system to the inertial-axis reference system. This was done by the computer for six degrees of freedom. The necessary equations and their derivations are given in references 2 and 3.

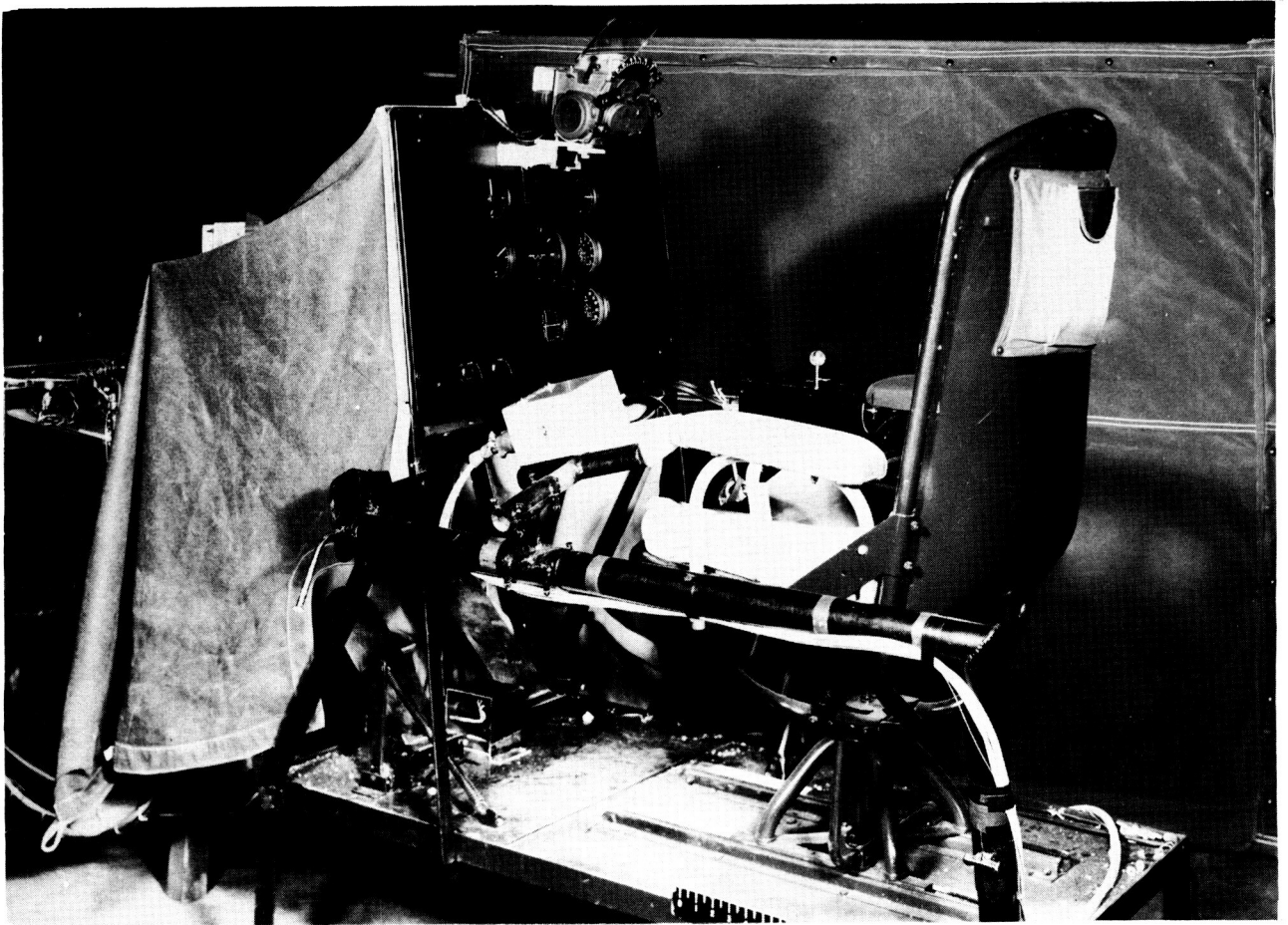


Figure 1.- Photograph of simulator cockpit.

L-61-2652

Figure 3 illustrates the line-of-sight relations between the station and ferry. The angle  $\alpha$  lies between the line of sight and the horizontal ( $X_i Y_i$ ) plane;  $\beta$  is the angle between the orbital ( $X_i Z_i$ ) plane and the line of sight. From the figure it can be seen that:

$$\beta = \tan^{-1} \frac{y_i}{x_i} \quad (1)$$

$$\alpha = \tan^{-1} \frac{z_i}{\sqrt{x_i^2 + y_i^2}} \quad (2)$$

$$R = \sqrt{x_i^2 + y_i^2 + z_i^2} \quad (3)$$

## Radar Presentation

The tests were based on data from an early airborne tracking radar system. The system was assumed to have a root-mean-square tracking error of 2.7 milliradians and an autocorrelation function given by

$$\lambda_R = 7.29e^{-2.50t} \text{ milliradians}^2 \quad (4)$$

A comparison of radar noise and the noise-generator output showing the actual value of noise corresponding to the angle-tracking noise, and the noise level after differentiation, is given in the appendix.

## Noise Generator

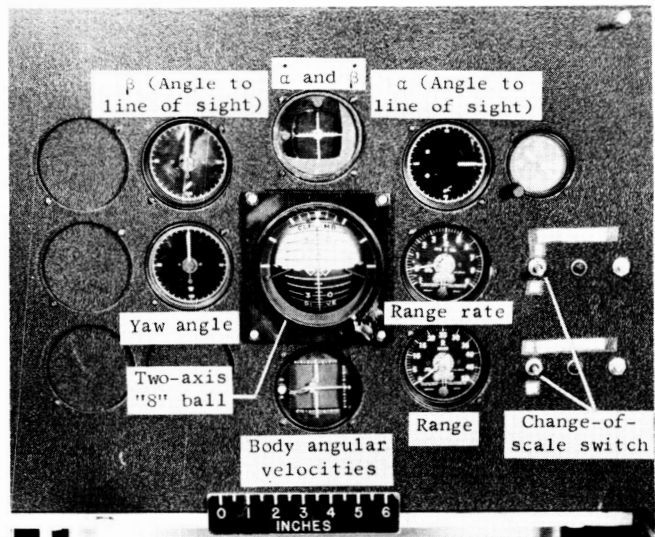
The radar noise was simulated by a one-channel random-noise generator, filtered to give an autocorrelation of

$$\lambda_G = Ke^{-2.50t} \text{ milliradians}^2 \quad (5)$$

where  $K$  is a constant which was determined by a potentiometer setting in the analog computer.

Although the angle-tracking noise should appear in  $\alpha$  and  $\beta$ , the 2.7-milliradian error was not impressed on the line-of-sight angle display because a resolution of only about 5 milliradians was required for the rendezvous. The largest error occurred in the more critical angular-rate presentation. To determine the angular rates  $\dot{\alpha}$  and  $\dot{\beta}$ , both line-of-sight angle and noise corresponding to the radar angle-tracking output were fed into an approximate differentiation circuit. The output was the angular rates and their corresponding noise overlays. This output was then fed into a low-pass filter and out of the filter to the instrument display.

With the angle-tracking error assumed, the rate signal obtained would have had noise peaks much greater than the maximum range of the rate meter. Therefore, rather heavy filtering of this signal was required to make it usable. The exact filtering time constant required is a subject for further investigation, but is beyond the scope of this study. For this study a 5-second filter time constant was chosen to smooth the noise peaks and to prevent self-oscillation of the analog circuit. With this level of filtering, occasional noise peaks could deflect the  $\dot{\alpha}$  and  $\dot{\beta}$  needles full scale at maximum sensitivity.



L-60-4266.1  
Figure 2.- Cockpit instruments.

## TESTS

The pilot-controlled simulator used in the present radar-noise study was placed in a closed-loop system linked through an analog computer. Initial conditions were fed to the cockpit instruments from the computer. The pilot's displacement and attitude corrections were then fed back to the computer, which

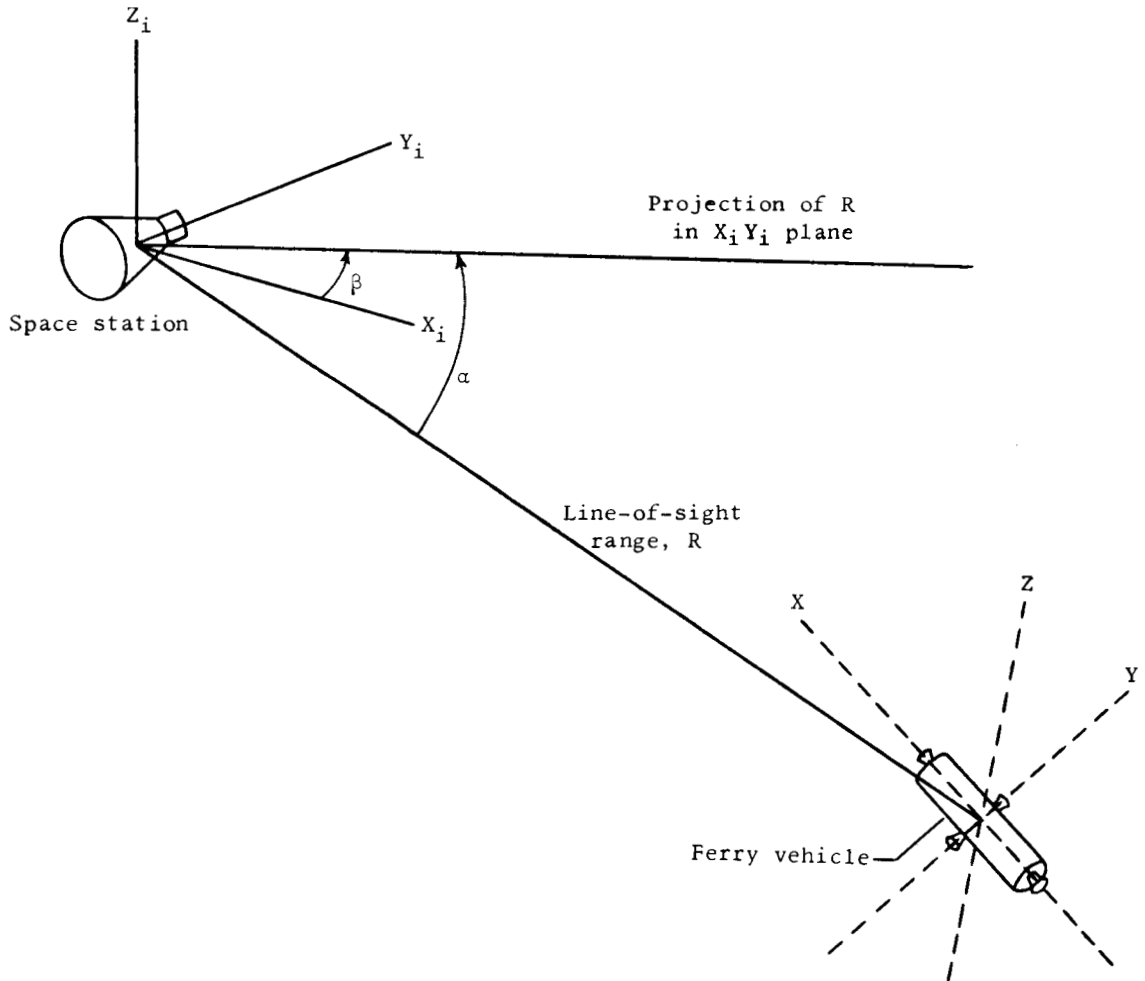


Figure 3.- Line-of-sight and Euler angle relations between ferry vehicle and space station.

solved the equations of motion and fed the new data back to the instruments, completing the system loop. The data required by the pilot were range and range rate, line-of-sight angles and rates, and attitude of the controlled vehicle. The ferry vehicle was assumed to have a pair of right-left transverse rockets and a pair of fore-and-aft longitudinal rockets for main thrusting, and smaller variable-thrust attitude rockets. Translational control was provided by four pushbuttons which operated the main rockets in an on-off manner. Rudder treadles and a two-axis side-arm controller were used in a rate-command attitude-control system with a 4-second time constant and maximum acceleration of  $0.05 \text{ radian/sec}^2$ .

The maximum initial conditions investigated were: range, 50 miles; range rate, 1,000 ft/sec; line-of-sight angles,  $\pm 45^\circ$ ; line-of-sight angle rates,  $\pm 15$  milliradians/sec. Except for the noise-induced errors in the  $\dot{\alpha}$  and  $\dot{\beta}$  presentation, all instrumentation was considered perfect. No thrust misalignment was assumed.

The simulations were flown by three pilots, two NASA test pilots and a research engineer who was formerly a military pilot. The first series of tests was made with no noise in the instrument display. After the pilots had become proficient in the rendezvous technique, noise was introduced into the display for the second series of tests.

Starting from any particular set of initial conditions, the pilot was to achieve an intercept, or collision, course as soon as possible, and hold the course while reducing range and range rate to zero. The only conditions necessary to fix the course are:

$$\dot{R} \text{ is negative} \qquad \dot{\alpha} = 0 \qquad \dot{\beta} = 0$$

Little excess fuel is used if the pilot establishes the initial collision course quickly and accurately.

In order for the pilot to set the initial interception course in the present tests, it was necessary for him to determine the true line-of-sight rates by functioning in a manner analogous to an integrator. He had to sum all the impulses of the indicator mentally and take their mean to obtain the true value. One unrealistic condition encountered in the simulation was the single channel of noise, which caused the noise deflection of the  $\dot{\alpha}$  needle to be the same as that of the  $\dot{\beta}$  needle and made it somewhat easier to find the mean of both simultaneously. However, the design of the meter (fig. 2) increased the difficulty somewhat by forcing the pilot to observe  $\dot{\alpha}$  sweeping vertically and  $\dot{\beta}$  sweeping horizontally.

## RESULTS AND DISCUSSION

The tests show that an experienced pilot could successfully complete the terminal phase of space rendezvous in the presence of the filtered radar noise that was simulated in this investigation, but only with a sacrifice of time and fuel. The additional difficulty, and therefore the extra fuel required, was apparently constant for any particular root-mean-square noise level, although total fuel consumption varied with initial conditions. The factor that influenced the pilot's ability to control the maneuver accurately during the early phases of the rendezvous was the noise amplitude; the greater the amplitude, the larger the uncertainty of the mean instrument reading. Not only was the maneuver more difficult with noise, but pilots tended to be less positive that they were making the proper correction. This has been verified in tests with a fighter-plane fire-control system (ref. 4).



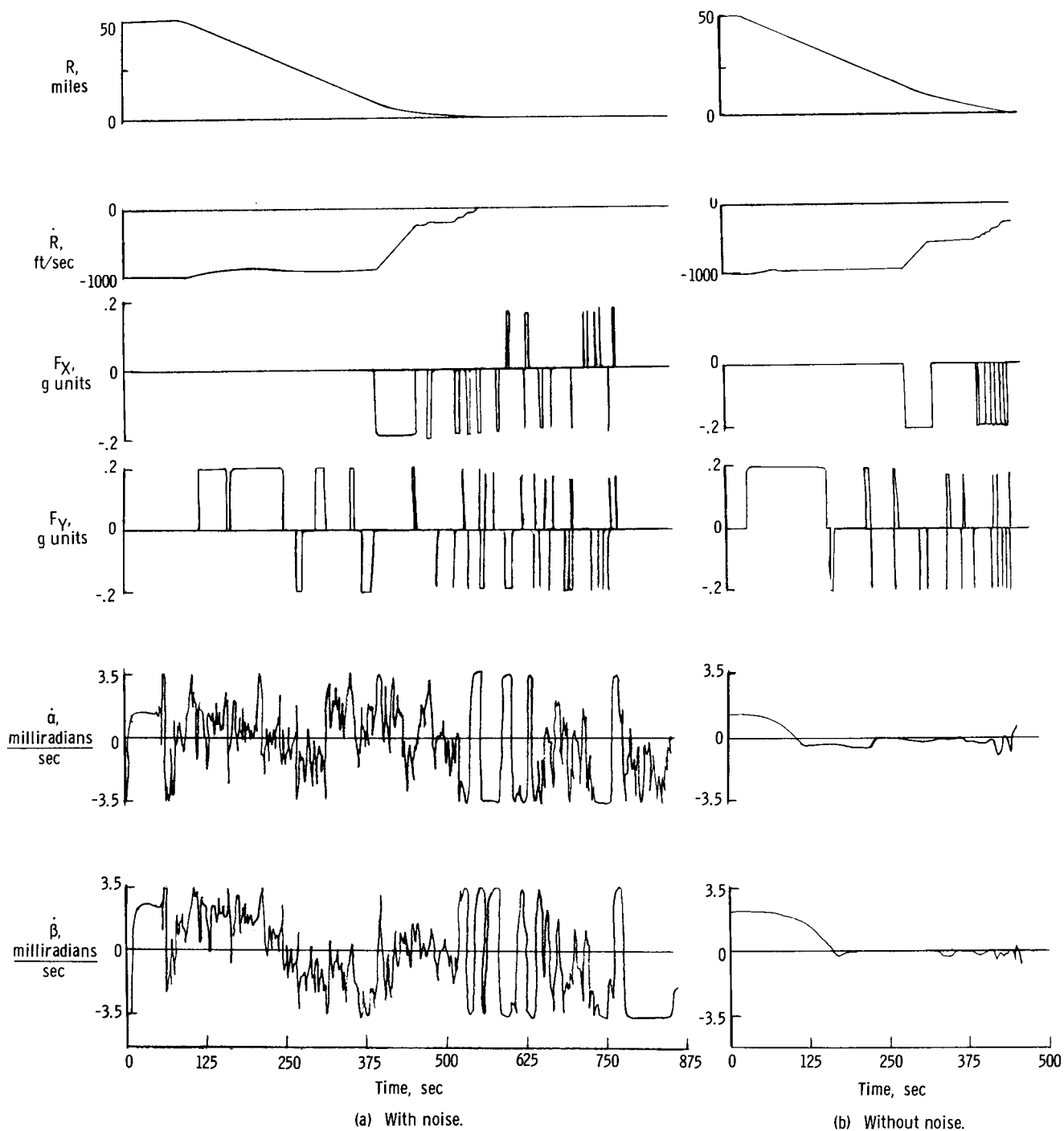


Figure 4.- Time history of rendezvous.

A comparison of noise and no-noise runs is made in the analog recording shown in figure 4. The indeterminacy of the tracking signal caused by the addition of the noise is readily apparent. Integration of the force-time curves of figure 4 gives the product of acceleration and time, or the characteristic velocity for the maneuver, and shows that the fuel consumption increases with the time required to perform the maneuver. For example, a typical no-noise run had a characteristic velocity of 1,411.3 ft/sec, whereas the same run with noise had a characteristic velocity of 2,025.4 ft/sec, resulting in a 43.5-percent increase in thrusting fuel. In addition excess attitude-rocket fuel, which was not recorded, would boost this figure.

A more direct way to show the increased difficulty caused by the radar noise would be to compare the distances traveled while performing the same task with and without radar-noise background. Figure 5 presents this comparison for noise with a root-mean-square value of 0.52 milliradian/sec. Tests with lower noise amplitudes produced distance trajectories with closer agreement, but any perceptible noise level was characterized by some effect on the pilot's control.

Since the line-of-sight angle rates are inversely proportional to the range, a condition which would produce a small change in  $\dot{\alpha}$  and  $\dot{\beta}$  at the beginning of the rendezvous would cause a large change at close range. The 5-second filter time constant used in this study caused difficulty during the final closing and braking phase by introducing a lag between the change in the rates and the display on the instruments. Although a larger filter time constant would have smoothed the noise peaks more and made the initial phases of rendezvous easier, it would also increase the display lag in the final phases. The difficulty presented by the lag is apparent in figure 4(a), in which almost a third of the mission time was required to complete the final few miles of closure. This indicates that while higher filtering is desirable during the early phases of rendezvous, a lower filtering level is necessary during the final phases.

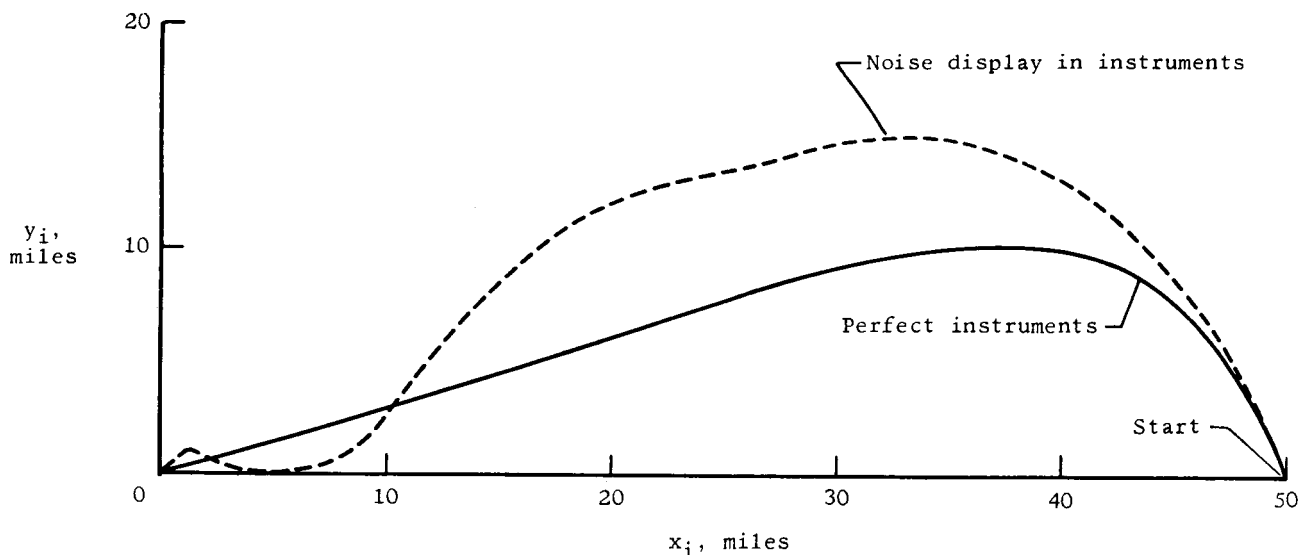


Figure 5.- Typical rendezvous with and without noise in instrument displays.

## CONCLUDING REMARKS

An investigation has been conducted to determine the effects of radar noise on the pilot's ability to complete the terminal phase of space rendezvous. The presentation of the noise signal on the line-of-sight angular-rate instruments was chosen as representative of the most critical source of error. The early accuracy needed in these measurements is greatest, and the entire maneuver depends upon the successful use of these rate data.

The results showed that the pilot's efficiency decreased with increase in noise amplitude. However, he was able to complete the mission in all cases, even when the simulated noise was more severe than that to be expected from current systems.

The results indicate that a variation of the filter time constant with range would be desirable. A large filter time constant is necessary to smooth the noise peaks during the tracking and initial braking phases, while a small time constant is necessary at close range to avoid a lag in the data display. The 5-second filter time constant used in this study would fall somewhere between these limits.

Langley Research Center,  
National Aeronautics and Space Administration,  
Langley Station, Hampton, Va., December 19, 1962.

## APPENDIX

### EQUATIONS AND CALCULATIONS

Figure 6 is a block diagram of the noise-generator circuit. In order to make the test conditions as realistic as possible, the noise signal was impressed on the line-of-sight angle signal before differentiation. With this procedure the actual value of noise corresponding to the tracking error could be inserted, and the noise level after passing through the differentiating circuit was the

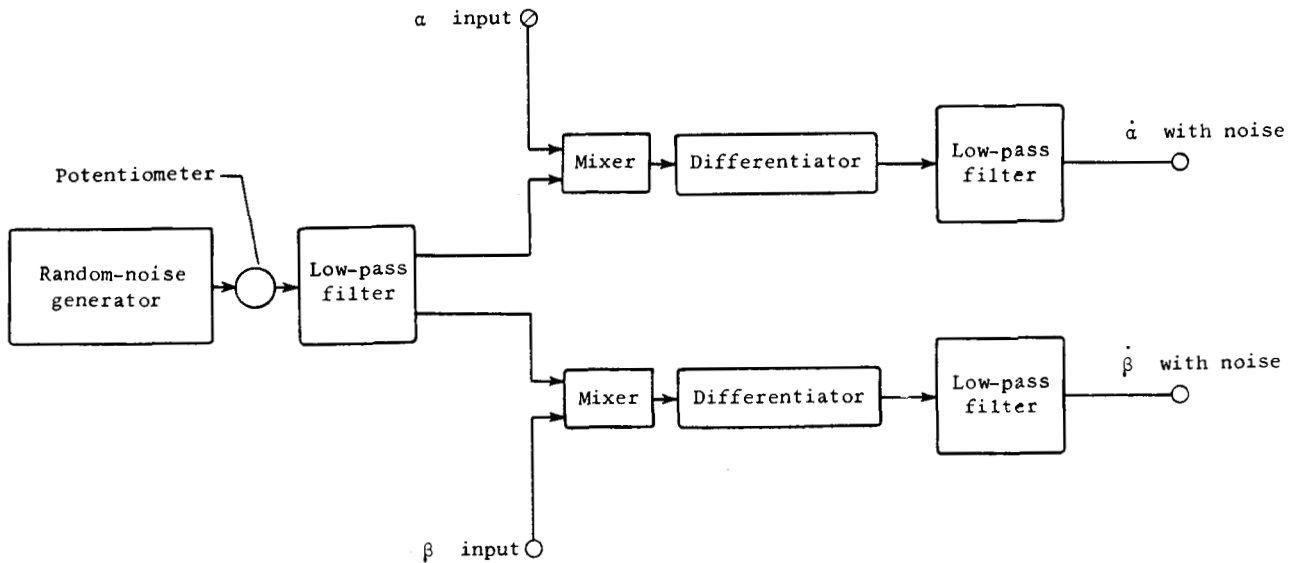


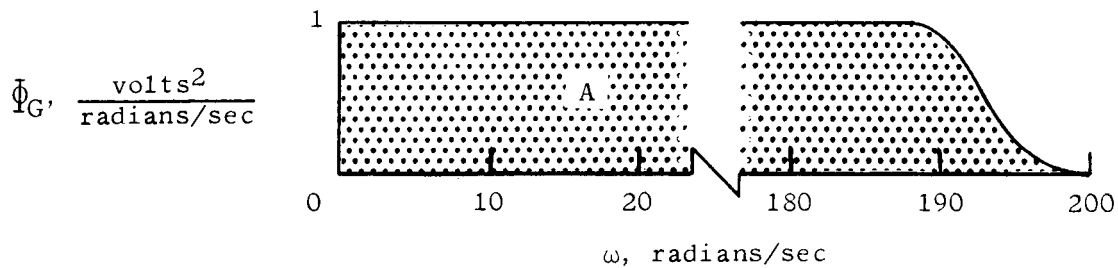
Figure 6.- Block diagram of radar noise simulator.

value which could be expected from differentiation in a radar system. However, for the study to be meaningful it was necessary to determine the angle-rate error obtained as a function of the angle error differentiated. This was accomplished by an analytical comparison of error outputs.

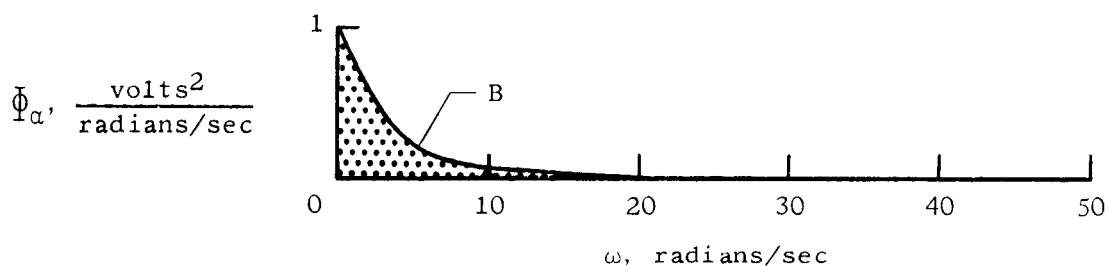
### Power Spectral Densities

Figure 7(a) shows the power-spectral-density curve of the noise as it came from the random-noise generator. The output is constant to about 30 cps and then drops off sharply. The area A under the curve is  $\sigma^2$ , the mean-square value of the noise signal. After passing through a low-pass filter with a time constant  $\tau$  the noise has a power spectral density given by

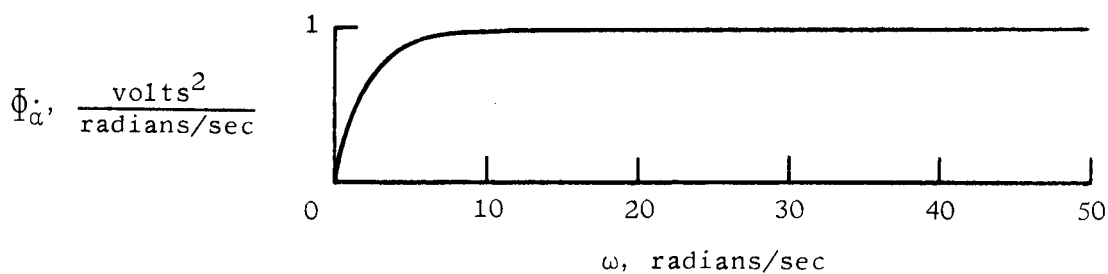
$$\Phi_{\alpha} = \frac{1}{1 + \tau^2 \omega^2} \text{ volts}^2 \quad (6)$$



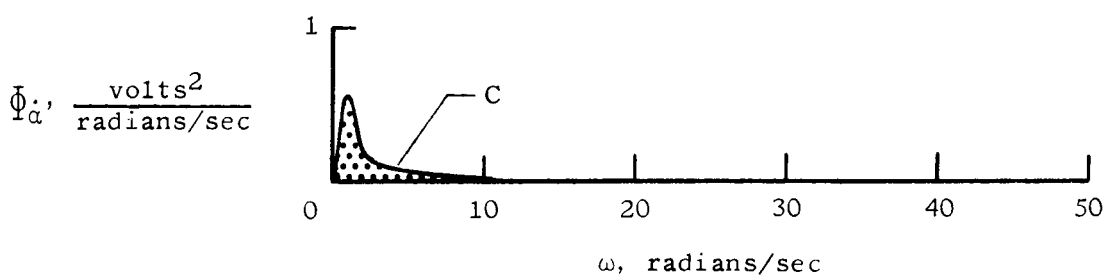
(a) Noise-generator output.



(b) Low-pass filter output.



(c) Differentiator output.



(d) Low-pass filter output.

Figure 7.- Power curves of noise circuit.

The new function has the curve shown in figure 7(b). The initial value of  $\Phi$  was assumed to be unity; that is not exactly true, but since only the ratios of the areas are involved in the calculations, no error is introduced by this assumption. The area B under the curve is the mean-square value of  $\alpha$  or  $\beta$ . After differentiation with respect to time, equation (6) becomes

$$\Phi_{\dot{\alpha}} = \frac{\omega^2}{1 + \tau^2 \omega^2} \text{ volts}^2 \quad (7)$$

and the corresponding curve is shown in figure 7(c). The output of the differentiator was then passed through a low-pass filter with time constant  $\tau_2$  to smooth the differentiated signal. The output signal from the low-pass filter is given by

$$\Phi_{\dot{\alpha}} = \left( \frac{\omega^2}{1 + \tau^2 \omega^2} \right) \left( \frac{1}{1 + \tau_2^2 \omega^2} \right) \quad (8)$$

The area C under the resulting curve (fig. 7(d)) is the mean-square value of  $\dot{\alpha}$ . The actual root-mean-square values of  $\alpha$  and  $\dot{\alpha}$  can be found by relating areas B and C.

#### Equations for Areas

The areas can be determined by employing the Cauchy residue theorem, which states that the integral of a function over a contour containing within it only isolated singular points of the function is equal to  $2\pi i$  times the sum of the residue of these points.

For area B:

$$\sigma_{\alpha}^2 = \int_{-\infty}^{\infty} \frac{1}{1 + \tau^2 \omega^2} d\omega = \int_{-\infty}^{\infty} \frac{d\omega}{(1 + \tau i \omega)(1 - \tau i \omega)} \quad (9)$$

Let

$$s = i\omega \quad ds = i d\omega \quad d\omega = -i ds$$

Then

$$\sigma_{\alpha}^2 = -i \int_{-i\infty}^{i\infty} \frac{ds}{(1 + \tau i \omega)(1 - \tau i \omega)} = -i \int_{-i\infty}^{i\infty} \frac{ds}{\tau^2 \left( \frac{1}{\tau} + s \right) \left( \frac{1}{\tau} - s \right)}$$

If  $s = -1/\tau$ , the residue is

$$K_{-1/\tau} = \left. \frac{1}{\tau^2 \left( \frac{1}{\tau} - s \right)} \right]_{s=-1/\tau} = \frac{1}{\tau^2 \frac{2}{\tau}} = \frac{1}{2\tau} \quad (10)$$

The value of the integral is  $2\pi \frac{1}{2\tau}$ .

For area C:

$$\sigma_{\dot{\alpha}}^2 = \int_{-\infty}^{\infty} \frac{1}{1 + \tau_2^2 \omega^2} \frac{\omega^2}{1 + \tau^2 \omega^2} d\omega \quad (11)$$

Let  $s = i\omega$ ; then

$$\sigma_{\dot{\alpha}}^2 = -i \int_{-i\infty}^{i\infty} \frac{-s^2 ds}{\tau^2 \tau_2^2 \left( \frac{1}{\tau} + s \right) \left( \frac{1}{\tau} - s \right) \left( \frac{1}{\tau_2} + s \right) \left( \frac{1}{\tau_2} - s \right)}$$

$$\begin{aligned} K_1 &= K_{-1/\tau} \\ &= \left. \frac{-s^2}{\tau^2 \tau_2^2 \left( \frac{1}{\tau} - s \right) \left( \frac{1}{\tau_2} + s \right) \left( \frac{1}{\tau_2} - s \right)} \right]_{s=-1/\tau} \\ &= \frac{-1}{\tau^4 \tau_2^2 \left( \frac{2}{\tau} \right) \left( \frac{1}{\tau_2} - \frac{1}{\tau} \right) \left( \frac{1}{\tau_2} + \frac{1}{\tau} \right)} \end{aligned} \quad (12)$$

$$\begin{aligned} K_2 &= K_{-1/\tau_2} \\ &= \left. \frac{-s^2}{\tau_2^2 \tau^2 \left( \frac{1}{\tau} + s \right) \left( \frac{1}{\tau} - s \right) \left( \frac{1}{\tau_2} - s \right)} \right]_{s=-1/\tau_2} \\ &= \frac{-1}{\tau_2^4 \tau^2 \left( \frac{1}{\tau} - \frac{1}{\tau_2} \right) \left( \frac{1}{\tau} + \frac{1}{\tau_2} \right) \frac{2}{\tau_2}} \end{aligned} \quad (13)$$

$$\begin{aligned} K &= K_1 + K_2 \\ &= \frac{-1}{2\tau(\tau - \tau_2)(\tau + \tau_2)} + \frac{-1}{2\tau_2(\tau_2 - \tau)(\tau_2 + \tau)} \end{aligned} \quad (14)$$

The value of the integral is  $2\pi K$ .

### Numerical Evaluation

Area B: For this area,  $\tau = 0.4$  second. Therefore

$$B = 2\pi \frac{1}{2\tau} = 6.28 \frac{1}{(2)(0.4)} = 7.85 \text{ volts}^2$$

Since the  $\alpha$  and  $\beta$  meters were scaled to 2 degrees/volt,

$$\sigma_{\alpha} = 3.29^{\circ} = 57.3 \text{ milliradians}$$

Area C: For this area,  $\tau_2 = 5.0$  seconds. Thus

$$\sigma_{\dot{\alpha}}^2 = C = 2\pi(0.0503 - 0.0403) = 0.291 \text{ volts}^2/\text{sec}^2$$

The ratio of C to B is  $\frac{\text{volts}^2/\text{sec}^2}{\text{volts}^2}$ . Then

$$\sqrt{\frac{0.291}{7.85}} 57.3 = (0.193)(57.3) = 11.05 \text{ milliradians/sec}$$

The  $\dot{\alpha}$  and  $\dot{\beta}$  meter was arranged for a full-scale reading of 1.5 milliradians/sec in order to aid the pilot in following a collision course closely. The simulated root-mean-square error signal in  $\alpha$  of 2.7 milliradians therefore gave a root-mean-square error signal in  $\dot{\alpha}$  of  $(0.193)(2.7) = 0.52$  milliradian/sec.



## REFERENCES

1. Lineberry, Edgar C., Jr., Brissenden, Roy F., and Kurbjun, Max C.: Analytical and Preliminary Simulation Study of a Pilot's Ability to Control the Terminal Phase of a Rendezvous With Simple Optical Devices and a Timer. NASA TN D-965, 1961.
2. Brissenden, Roy F., Burton, Bert B., Foudriat, Edwin C., and Whitten, James B.: Analog Simulation of a Pilot-Controlled Rendezvous. NASA TN D-747, 1961.
3. Hord, Richard A.: Relative Motion in the Terminal Phase of Interception of a Satellite or a Ballistic Missile. NACA TN 4399, 1958.
4. Briggs, George E., and Fitts, Paul M.: Tracking Proficiency as a Function of Visual Noise in the Feedback Loop of a Simulated Radar Fire Control System. Res. Rep. AFPTRC-TN-56-134, ASTIA Doc. No. 098911, Air Res. and Dev. Command, Dec. 1956.